



1 **Climate information preserved in seasonal water isotope at**  
2 **NEEM: relationships with temperature, circulation and sea**  
3 **ice**  
4

5 Minjie Zheng<sup>1\*</sup>, Jesper Sjolte<sup>1</sup>, Florian Adolphi<sup>1,2</sup>, Bo Møllersøe Vinther<sup>3</sup>, Hans Christian  
6 Steen-Larsen<sup>4</sup>, Trevor James Popp<sup>3</sup>, and Raimund Muscheler<sup>1</sup>

7 <sup>1</sup>Department of Geology, Quaternary Science, Lund University, Lund, Sweden

8 <sup>2</sup>Climate and Environmental Physics, Physics Institute, and Oeschger Centre for Climate Change Research,  
9 University of Bern

10 <sup>3</sup>Centre for Ice and Climate, Niels Bohr Institute, University of Copenhagen, Copenhagen, Denmark

11 <sup>4</sup>Geophysical Institute and Bjerknes Centre for Climate Research, University of Bergen, Norway

12

13 *Correspondence to: Minjie Zheng (minjie.zheng@geol.lu.se)*

14 **Abstract**

15 Analyzing seasonally resolved  $\delta^{18}\text{O}$  ice core data can aid the interpretation of the climate information in  
16 ice cores, providing also insights into factors governing the  $\delta^{18}\text{O}$  signal that cannot be deciphered by  
17 investigating the annual  $\delta^{18}\text{O}$  data only. However, the seasonal isotope signal has not yet to be investigated in  
18 northern Greenland, e.g. at the NEEM (North Greenland Eemian Ice Drilling) ice core drill site. Here we analyze  
19 seasonally resolved  $\delta^{18}\text{O}$  data from four shallow NEEM ice cores covering the last 150 years. Based on  
20 correlation analysis with observed temperature, we attribute about 70% and 30 % of annual accumulation to  
21 summer and winter respectively. The NEEM summer  $\delta^{18}\text{O}$  signal correlates strongly with summer western  
22 Greenland coastal temperature and with the first principal component (PC1) of summer  $\delta^{18}\text{O}$  from multiple  
23 seasonally resolved ice cores from central/southern Greenland. However, there are no significant correlations  
24 between NEEM winter  $\delta^{18}\text{O}$  data and western Greenland coastal winter temperature, or southern/central  
25 Greenland winter  $\delta^{18}\text{O}$  PC1. The stronger correlation with temperature during summer and the dominance of  
26 summer precipitation skew the annual  $\delta^{18}\text{O}$  signal in NEEM. The strong footprint of temperature in NEEM  
27 summer  $\delta^{18}\text{O}$  record also suggests that the summer  $\delta^{18}\text{O}$  record, rather than the winter  $\delta^{18}\text{O}$  record, is a better  
28 temperature proxy at the NEEM site. Despite dominant signal of North Atlantic Oscillation (NAO) and Atlantic  
29 Multidecadal Oscillation (AMO) in the central-southern ice cores data, both NAO and AMO exert weak  
30 influences on NEEM seasonal  $\delta^{18}\text{O}$  variations. The NEEM seasonal  $\delta^{18}\text{O}$  is found to be highly correlated with  
31 Baffin Bay sea ice concentration (SIC) in satellite observation period (1979-2004), suggesting a connection of  
32 the sea ice extent with  $\delta^{18}\text{O}$  at NEEM. NEEM winter  $\delta^{18}\text{O}$  significantly correlates with SIC even for the period  
33 prior to satellite observation (1901-1978). The NEEM winter  $\delta^{18}\text{O}$  may reflect sea ice variations of Baffin Bay  
34 rather than temperature itself. This study shows that seasonally resolved  $\delta^{18}\text{O}$  records, especially for sites with  
35 seasonal precipitation bias such as NEEM, provide a better understanding of how changing air temperature and  
36 circulation patterns are associated with the variability of the  $\delta^{18}\text{O}$  records.

37



## 38 1. Introduction

39 Stable water isotopes in Greenland ice cores, e.g.  $\delta^{18}\text{O}$ , provide key information on temperature (Küttel et al., 2012), moisture source (Masson-Delmotte et al., 2005b), sea ice extent (Noone and Simmonds, 2004) or atmospheric circulation (Vinther et al., 2003). The available data have revealed the complexity of the integrated information preserved in the stable water isotope composition of Greenland ice cores (Masson-Delmotte et al., 2005a), thereby illustrating the need for improving our understanding of its climatic controls. Recent studies indicate that having not only the annual, but seasonally resolved ice core  $\delta^{18}\text{O}$  data, represents a significant improvement for the interpretation of the  $\delta^{18}\text{O}$  signal (Vinther et al., 2003; Vinther et al., 2010). For example, Ortega et al. (2014) indicated that the seasonal  $\delta^{18}\text{O}$  records allow to reconstruct the variability of weather regimes in the North Atlantic region.

48 Vinther et al. (2010) extracted the seasonal  $\delta^{18}\text{O}$  from 13 ice cores in central and southern Greenland. However, seasonally resolved data are still lacking from northern Greenland, for example, the NEEM (North Greenland Eemian Ice Drilling, 77.45° N, 51.06° W, 2450 m a.s.l., Fig. 1) ice core. The NEEM project originally aims to retrieve an ice core record spanning the last interglacial period (Neem community members, 2013). To assist interpreting the stable isotope record along the deep ice core, several shallow firn/ice cores were also drilled around the camp as part of the exploration program. Through investigating these short cores, the results suggest that the NEEM annually resolved  $\delta^{18}\text{O}$  records correlate unexpectedly weakly to the annual and winter North Atlantic Oscillation (NAO) signal (Steen-Larsen et al., 2011; Masson-Delmotte et al., 2015). This contrasts with  $\delta^{18}\text{O}$  records from central and southern part of Greenland that strongly correlate with the winter NAO signal (Vinther et al., 2003; Vinther et al., 2010). Regional to global atmospheric models show that precipitation at NEEM is dominated by summer precipitation, which may contribute to the lack of the winter NAO fingerprint in annual NEEM  $\delta^{18}\text{O}$  records (Steen-Larsen et al., 2011). This seasonal precipitation bias may skew the annual  $\delta^{18}\text{O}$  signal towards summer precipitation and cause a weak correlation to the NAO which exerts its strongest influence on Greenland weather in winter. Indeed, there is no explanation yet for the strong correlation between the first principal component (PC1) of 16 annually resolved Greenland  $\delta^{18}\text{O}$  records and NEEM annual  $\delta^{18}\text{O}$  records despite the missing NAO fingerprint in NEEM data (Masson-Delmotte et al., 2015). Furthermore, Steen-Larsen et al. (2011) found that the annual sea ice extent anomaly in the Baffin Bay explains up to 34% of variations of the annual NEEM  $\delta^{18}\text{O}$  record. Hence, studying seasonally resolved NEEM  $\delta^{18}\text{O}$  might help us to explore the possible seasonal relationship with the Baffin Bay ice concentration.

67 In this study, we follow the approach of Vinther et al. (2010) to extract the winter and summer  $\delta^{18}\text{O}$  signal from four NEEM short cores. To reduce noise, the records are averaged for the overlap period from 1855 to 2004 C.E. We then compare the seasonal  $\delta^{18}\text{O}$  NEEM record with other seasonal  $\delta^{18}\text{O}$  records from central and southern Greenland and their first principle component (PC1) (Vinther et al., 2010). Meteorological parameters like temperature and sea level pressure are also compared with the NEEM seasonal  $\delta^{18}\text{O}$  data to explore temporal and spatial relationships. The Baffin Bay sea ice concentration (SIC) data covering both the satellite period (1979-2004) and the period prior to satellite observation (1901-1978), are also compared with NEEM  $\delta^{18}\text{O}$  data. The aim is to identify the seasonal  $\delta^{18}\text{O}$  signal at NEEM and to investigate which parameters control the NEEM  $\delta^{18}\text{O}$  variations for each season in terms of seasonal weather/climate variability.

76



77 **2. Meteorological data**

78 **2.1 Temperature records**

79 The length of observational records and locations of meteorological stations are crucial for a robust  
80 correlation between ice cores and meteorological observations. The Pituffik station is the only observation  
81 station in the northwestern part of Greenland (NW Greenland) and the closest one to the NEEM site (Fig.1;  
82 Cappelen, 2017). Although the temperature record only covers the period back to 1948, the Pituffik station is the  
83 best source of information on the weather and climate in NW Greenland. As the ice core data spans the last 150  
84 years, we also test our  $\delta^{18}\text{O}$  record against longer-term temperature observations from southwestern part of  
85 Greenland (SW Greenland). The SW Greenland temperature record is a merged temperature dataset based on 13  
86 observational records along the southwestern Greenland coastal area spanning the period 1784-2005 (Fig.1;  
87 Vinther et al., 2006). This data set covers the complete period of seasonally resolved ice core isotope data from  
88 NEEM facilitating an extended comparison period. The changes in NW Greenland coastal temperatures are  
89 regionally consistent around western coastal Greenland (Hanna et al., 2012; Wong et al., 2015). Therefore, some  
90 consistency of the SW Greenland temperature record with temperatures closer to NEEM can be expected.

91 **2.2 Twenty Century Reanalysis data**

92 The Twenty Century Reanalysis (20CR; Compo et al., 2011) data set is selected to investigate the  
93 relationship between NEEM isotope records and atmospheric circulation patterns and temperature. The 20CR  
94 data is a global atmospheric 2 by 2 degree gridded climate model dataset only assimilating surface observations  
95 of synoptic pressure, and using sea surface temperature and sea ice concentration as boundary conditions  
96 (Compo et al., 2011). This dataset provides estimates of global atmospheric variability spanning 1851 to 2012 at  
97 six-hourly resolution. However, there are very few stations delivering pressure data over the Greenland area until  
98 1922 after which the number of observation stations increases significantly (Compo et al., 2011). This leads to a  
99 less well-constrained reanalysis data set for the Greenland for the period before 1930. To test the results for the  
100 early period, we divide the whole period into two subperiods 1855-1930 and 1931-2004 and examine  
101 correlations to ice core data within these subperiods. The aim is to investigate the influence of temperature and  
102 atmospheric circulation on NEEM seasonal  $\delta^{18}\text{O}$  signals.

103 **2.3 Indices of climate patterns**

104 Previous analyses have related the variability in the Greenland ice core stable water isotopes to changes  
105 in the atmospheric North Atlantic Oscillation (NAO; Barlow et al., 1993; Vinther et al., 2003) and the oceanic  
106 Atlantic Multidecadal Oscillation (AMO; Chylek et al., 2012). In this study, these two indices are extracted from  
107 the 20CR dataset. We choose the PC-based NAO (NAOPC) indices which optimally represents the NAO pattern  
108 spatially and temporally (Hurrell and Deser, 2009). To obtain the monthly NAOPC index, we performed the  
109 empirical orthogonal function (EOF) on monthly pressure anomalies over the Atlantic sector, 20°-80°N, 90°W-  
110 40°E. The leading mode of EOF is used as the monthly NAOPC index. For the AMO index, we first average the  
111 sea surface temperature anomalies over the sector 0°-60°N, 0°-80°W then subtract the average sea surface  
112 temperature anomalies between 60°S-60°N from it (Trenberth and Shea, 2006). By calculating indices from the  
113 20CR data, both indices can cover the period 1855-2004.

114



## 115 **2.4 Baffin Bay ice concentration**

116 Steen-Larsen et al. (2011) suggested a strong link between annual sea ice cover in Baffin Bay and NEEM  
117 annual  $\delta^{18}\text{O}$  signal. To test this hypothesis, we selected the COBESic sea ice data set to compare with the NEEM  
118 seasonal  $\delta^{18}\text{O}$  data. The COBESic record (Hirahara et al., 2014) is a combination of monthly globally complete  
119 fields of sea ice concentration on a 1 by 1 degree grid based on satellite observation starting after 1979 and  
120 historical data provided by Walsh and Chapman (2001). The mean Baffin Bay area sea ice concentration was  
121 calculated by averaging the values over the area between 65-80° N and 80-50° W (Tang et al., 2004).

## 122 **3 Ice core data**

### 123 **3.1 The NEEM shallow ice core data**

124 The annual  $\delta^{18}\text{O}$  data from four shallow NEEM ice cores (NEEM07S3; NEEM08S2; NEEM08S3;  
125 NEEM10S2) have been published by Masson-Delmotte et al. (2015). The shallow cores cover depths ranging  
126 from the surface down to between 52.6 and 85.3 m. A back-diffusion calculation following Johnsen et al. (2000)  
127 was applied to the  $\delta^{18}\text{O}$  records to restore the original variability and hence, improve the identification of  
128 individual years. The annual dating of those records was performed by counting the seasonal cycles in  $\delta^{18}\text{O}$  and  
129 verified by identifying signals of volcanic eruptions in the electrical conductivity measurements (Masson-  
130 Delmotte et al., 2015). The four shallow cores share a common period from 1855-2004 which is focus in this  
131 study.

### 132 **3.2 Greenland seasonal $\delta^{18}\text{O}$ data**

133 The NEEM seasonal  $\delta^{18}\text{O}$  data are also compared with other seasonal records obtained from 13 sites in  
134 central and southern Greenland over the period 1778-1970 (Fig.1; Vinther et al., 2010). Most records originate  
135 from single ice core while some are stacked records from multiple cores (GRIP, n=6; DYE3-71/79, n=2). The  
136 first principal component (PC1) of these ice core data is considered as representative of the seasonal  $\delta^{18}\text{O}$  signal  
137 of central and southern Greenland. Vinther et al. (2010) divided the Greenland seasonal  $\delta^{18}\text{O}$  data into summer  
138 and winter season corresponding to May-Oct and Nov-Apr, respectively.

### 139 **4 The definition of seasonal $\delta^{18}\text{O}$ data**

140 To classify the seasons, we assume that the extremes in the seasonal cycle of the  $\delta^{18}\text{O}$  data correspond to  
141 the intra-annual temperature extremes (Vinther et al., 2010). According to the SW Greenland and Pituffik  
142 temperature records, summer temperature maxima and winter temperature minima usually occur in July/August  
143 and January/February, respectively. For summer, we assign the maxima  $\delta^{18}\text{O}$  within the selected year to  
144 July/August. For winter, the mid-winter is already defined as the onset of the annual layers by Masson-Delmotte  
145 et al. (2015) based on the analysis of a combination of ice core data. Based on their time scale, we define onset  
146 of the annual layer (mid-winter) to January/February. Here, we only investigate the winter and summer season as  
147 it is very hard to reliably pinpoint the spring and autumn in the  $\delta^{18}\text{O}$  record. Another essential prerequisite for the  
148 classification of seasons is the sufficient accumulation rate to guarantee a clear preservation of the seasonal cycle  
149 (no less than 20 cm ice accumulation per year; Johnsen et al., 2000). At NEEM the estimated accumulation rate  
150 is 21.6 cm yr<sup>-1</sup> for the period of 1725-2007 meeting this requirement (Gfeller et al., 2014).



151 The calculation of the summer mean  $\delta^{18}\text{O}$  is centered around the  $\delta^{18}\text{O}$  maxima value within the selected  
152 year. For the winter mean  $\delta^{18}\text{O}$  is centered around the onset of annual layer within the selected year. We then  
153 take different fractions of annual accumulation symmetrically around the seasonal center. This is done for four  
154 ice cores and these 4 seasonal  $\delta^{18}\text{O}$  series data are averaged to minimize noise. Finally, we correlate the averaged  
155 seasonal  $\delta^{18}\text{O}$  data to the winter and summer temperatures defined with different choices of season length.

156 Fig. 2 shows the result of the correlation analysis between different choices of winter and summer  
157 temperatures with different fractions of the NEEM annual  $\delta^{18}\text{O}$  signal. For SW Greenland and Pituffik summer  
158 temperature records (Fig. 2a and Fig. 2b), the highest correlations occur between May-October averaged  
159 temperature and a fraction of around 70% annual accumulation. In contrast, there is no significant correlation  
160 peak found when comparing NEEM winter  $\delta^{18}\text{O}$  with different choices of winter temperatures in NW and SW  
161 Greenland. However, it is interesting to note the correlation peak with the Pituffik temperature record in Fig. 2d  
162 at 30% annual accumulation, although not significant, which complements the result for the summer  
163  $\delta^{18}\text{O}$ /temperature correlation. For the winter signal the most significant correlation is obtained when the annual  
164 average SW Greenland temperature (Aug-Jul; Fig. 2c) is compared with annual average  $\delta^{18}\text{O}$  data (100% of the  
165 annual accumulation centered around the mid-winter). This significant correlation is likely due to the fact that  
166 the annually resolved  $\delta^{18}\text{O}$  includes the summer signal which indicates high correlation with annual average  
167 temperature that includes a strong imprint of the summer temperature. Furthermore, the correlation between  
168 NEEM winter  $\delta^{18}\text{O}$  data and SW Greenland temperature shows no correlation peak which is quite different from  
169 the one with the Pituffik record (Fig. 2d). The different relationships (Fig. 2c & Fig. 2d) suggest that the  
170 correlation between temperature and NEEM winter  $\delta^{18}\text{O}$  may vary for different periods. However, it should be  
171 noted that the Pituffik and SW Greenland temperature records represent different parts of Greenland climate over  
172 different time spans. We further examine the correlation between  $\delta^{18}\text{O}$  and SW Greenland temperature for 1949-  
173 2004 (Fig. S1, supplementary information). As expected, the correlation with SW Greenland over the period  
174 1949-2004 displays similar dependencies as the one shown in Fig. 2b & 2d for the Pituffik station, supporting  
175 the conclusion of a changing relationship between winter  $\delta^{18}\text{O}$  and Western Greenland temperatures over time.  
176 This weak and varied correlations of winter  $\delta^{18}\text{O}$  and temperature can likely be attributed to the intermittent and  
177 low winter precipitation at NEEM (Steen-Larsen et al., 2011). The correlation for SW Greenland during 1949-  
178 2004 shows the most significant correlation at higher annual accumulation for summer (80% for Apr-Nov) and  
179 lower for winter (peak at 20%). This result is consistent with the one indicated by Pituffik records.

180 Based on these results we conclude that, on average, about 70% of annual accumulation occurs between  
181 May-Oct, while the remaining 30% of annual accumulation occurs during Nov-Apr. We note that irrespectively  
182 of the actual process recording the  $\delta^{18}\text{O}$  in the snow being either precipitation weighted  $\delta^{18}\text{O}$ , a signal only  
183 driven by atmospheric water vapor isotopes as suggested by Steen-Larsen et al. (2014), or a combination our  
184 conclusion would still hold. An example of the chosen definition of seasons is shown in Fig. S2 (supplementary  
185 information). This conclusion is based on the strong and consistent correlation with two summer temperature  
186 data sets and the correlation peak for winter shown in Fig 2d. This conclusion is further supported by the  
187 comparison with the measured precipitation data in Pituffik station over the 1949-2000. Although the  
188 precipitation data are incomplete (almost no available data for 1976-1993), the average ratio of summer (May-  
189 Oct averaged) and winter (Nov-Apr averaged) precipitation over 1946-2000 is around 2 which is similar with



190 accumulation ratio in this study (summer/winter=2.3). This season definition also accords with seasonal  
191 classification in central and southern Greenland (Vinther et al., 2010).

192 Generally, the temperature imprint on NEEM  $\delta^{18}\text{O}$  is higher during summer than winter. The NEEM  
193 summer  $\delta^{18}\text{O}$ , rather than NEEM winter  $\delta^{18}\text{O}$ , is a better temperature proxy for the NEEM site and likely for  
194 northwestern Greenland. This result is in contrast to the finding that winter  $\delta^{18}\text{O}$  records in central/southern  
195 Greenland have been shown to be the better temperature proxy for past Greenland temperature conditions  
196 (Vinther et al., 2010). Therefore, one should be cautious when combining the NEEM seasonal  $\delta^{18}\text{O}$  with other ice  
197 cores data for use in temperature reconstructions. Another interesting feature is the dominant summer  
198 precipitation at the NEEM site (contributing to 70% of annual accumulation) compared to the ice cores in the  
199 central/southern Greenland (50% of annual accumulation for both season). Even though the investigated period  
200 only covers the last 150 yrs, knowing this seasonal variability can aid the climate interpretation of the long-term  
201  $\delta^{18}\text{O}$  variability. For example, climate model simulations suggest that seasonality changes over time with a  
202 decrease in winter precipitation during the glacial period, which would strongly affect sites with considerable  
203 winter accumulation, while being potentially less important for the sites, such as NEEM, with little winter  
204 accumulation (Werner et al., 2000).

## 205 **5 The seasonal $\delta^{18}\text{O}$ data**

### 206 **5.1 NEEM records and signal to noise ratio**

207 For low accumulation sites like NEEM, it is important to examine the signal to noise ratio (SNR; see  
208 Vinther et al. (2006) for a derivation of the SNR) in the  $\delta^{18}\text{O}$  data. The SNR for the  $\delta^{18}\text{O}$  data in NEEM cores is  
209 0.64 for the winter and 1.28 for the summer. The winter  $\delta^{18}\text{O}$  is more strongly influenced by noise than the  
210 summer signal possibly due to windier conditions and less snow accumulation. These two SNRs are in line with  
211 a previous study by Masson-Delmotte et al. (2015) that found a SNR of 1.3 for the annual NEEM  $\delta^{18}\text{O}$ . Note that  
212 the seasonal SNRs observed here are higher than the level obtained for six ice cores from the GRIP project (0.57  
213 for winter and 0.89 for summer; Vinther et al., 2010). Therefore, we conclude that the set of these four ice cores  
214 is sufficient to extract a robust seasonal  $\delta^{18}\text{O}$  at NEEM.

### 215 **5.2 Comparison with other Greenland ice core records**

216 Fig. 3 presents the correlation between seasonal stacked NEEM  $\delta^{18}\text{O}$  and other seasonal ice cores in  
217 Greenland, including the Greenland  $\delta^{18}\text{O}$  PC1. All data are detrended before correlation. The NEEM summer  
218  $\delta^{18}\text{O}$  data are significantly correlated with the summer Greenland ice core isotope data from locations in southern  
219 Greenland and to the west of the central ice divide (Fig. 3a; with correlation from 0.3 to 0.46). However, summer  
220  $\delta^{18}\text{O}$  from cores located to the east of the central ice divide (Renland, Site E, G and A) do not correlate  
221 significantly with the NEEM summer  $\delta^{18}\text{O}$  data. This is in accord with the fact that moisture pathways are  
222 different for snow accumulation to east and west of the central ice divide (Vinther et al., 2010). Therefore,  
223 having ice core records from both east and west side of the ice divide facilitates identification of regional-scale  
224 atmospheric variability. The correlation between NEEM summer  $\delta^{18}\text{O}$  and the Greenland summer PC1 record is  
225 significant both in inter-annual ( $r=0.54$ ) and 11-year smoothed data ( $r=0.67$ , Fig. 4a and c). The correlations of  
226 11-yr averaged data are tested using the 'Random-phase' method introduced by Ebisuzaki (1997). The  
227 correlations are consistent with the correlation between annual NEEM  $\delta^{18}\text{O}$  and Greenland  $\delta^{18}\text{O}$  PC1 found by



228 Masson-Delmotte et al. (2015). NEEM winter  $\delta^{18}\text{O}$  shows no significant correlation with most winter Greenland  
229  $\delta^{18}\text{O}$  records, and weak negative correlation with three southern ice core records (DYE3-71/79, 18C, 20D; Fig.  
230 3b). No correlations are observed for the comparison with Greenland winter  $\delta^{18}\text{O}$  PC1 at inter-annual and  
231 decadal scale (Fig. 4b and d). The results indicate a rather different winter climatic fingerprint archived in  
232 northwestern Greenland suggesting one needs to be careful when interpreting the NEEM winter  $\delta^{18}\text{O}$  records.  
233 Such poor correlations between NEEM winter  $\delta^{18}\text{O}$  and winter Greenland  $\delta^{18}\text{O}$  PC1 are obscured in the annual  
234 correlation with Greenland  $\delta^{18}\text{O}$  PC1 due to the dominance of summer accumulation (Masson-Delmotte et al.,  
235 2015).

## 236 **6 Comparison with regional climate**

### 237 **6.1 Association with the temperature and atmospheric circulation**

238 Fig. 5a and 5b show the spatial correlation maps between NEEM seasonal  $\delta^{18}\text{O}$  and surface air  
239 temperature (SAT) retrieved from the 20CR data set. All data are detrended before correlation. NEEM summer  
240  $\delta^{18}\text{O}$  is significantly positively correlated with May-Oct averaged SAT over all of Greenland, Baffin Bay and the  
241 open water to the east of Greenland. This significant correlation also occurs as far south as  $35^\circ\text{N}$  in the North  
242 Atlantic where a previous study suggests the possible moisture source for precipitation at NEEM (Steen-Larsen  
243 et al., 2011). For winter  $\delta^{18}\text{O}$  and Nov-Apr averaged SAT, no correlation is displayed over Greenland or nearby  
244 consistent with the results from observations. Winter  $\delta^{18}\text{O}$  correlates significantly with the SAT near  $35^\circ\text{N}$  in the  
245 North Atlantic and the Canadian Archipelago. But the correlation coefficients are only up to 0.25. Due to less  
246 reliable data in the early stage of 20CR data, we also examine the correlations within two sub-intervals 1855-  
247 1930 and 1931-2004 (Fig. S3). The strong extended correlations between NEEM summer  $\delta^{18}\text{O}$  and May-Oct  
248 averaged SAT are consistent within two sub-intervals. For winter correlations, both show no correlations over  
249 Greenland or nearby. The correlations with the SAT data from the reanalysis data support the conclusion that  
250 summer  $\delta^{18}\text{O}$  from NEEM has a better correlation with temperature than winter  $\delta^{18}\text{O}$ .

251 The NEEM seasonal  $\delta^{18}\text{O}$  is also compared with the sea level pressure (SLP) from 20CR data for the  
252 same time intervals as temperature (Fig. 5c, 5d and Fig. S4, supplementary information). There is no obvious  
253 NAO-like pattern (the seesaw structure over the North Atlantic Ocean) for the comparison between summer  $\delta^{18}\text{O}$   
254 and May-Oct averaged SLP for the whole period. A NAO-like pattern emerges for the second sub-period 1931-  
255 2004 (Fig S4b), but the northern node is limited suggesting a rather weak summer NAO footprint on  $\delta^{18}\text{O}$  at  
256 NEEM. There is a seesaw structure when correlating winter  $\delta^{18}\text{O}$  with Nov-Apr averaged SLP over the last 150  
257 yrs (Fig. 5d) and within the subperiod 1855-1930 (Fig. S4c). However, the correlations with SLP are also rather  
258 weak for these periods. The absolute values of correlation coefficients are less than 0.33 both for 1855-1930 and  
259 for whole period. Furthermore, it should be noted that there is an absence of the NAO-like pattern for the second  
260 75-year period (Fig. S4d) when observations are generally more reliable due to the increased number of  
261 assembled observations around Greenland. Hence, care should be taken when interpreting inconsistent  
262 correlations in the sub-intervals. Another interesting feature in Fig. S4c and S4d is the consistent negative  
263 correlation between NEEM winter  $\delta^{18}\text{O}$  and Nov-Apr averaged SLP over North America and Canadian  
264 Archipelago within the two subperiods. This suggests that NEEM winter  $\delta^{18}\text{O}$  is more likely influenced by the  
265 pressure over North America and Canadian Archipelago.





266 As the circulation indices are the simplified indicators of circulation patterns, we here further investigate  
267 the possible connections to AMO and NAO patterns with the seasonal NEEM data (Table 1). Both indices (Fig.  
268 4e and f) and NEEM seasonal data are detrended before correlation. The summer  $\delta^{18}\text{O}$  signal correlates weakly  
269 with May-Oct averaged AMO ( $r=0.22$ ) over 1855-2004. The correlations are also consistent within the two-  
270 subintervals. There is no correlation between winter  $\delta^{18}\text{O}$  and Nov-Apr averaged AMO. Summer  $\delta^{18}\text{O}$  correlates  
271 weakly with May-Oct averaged NAO over the whole period and for 1931-2004 but no correlation is seen in the  
272 1855-1930 period. It should be noted that for the whole period the summer correlation with NAO is significant,  
273 but no NAO-like pattern is seen in correlation with SLP for 1855-2004 (Fig. 5c). This may be attributed to the  
274 rather weak correlation with NAO which only is -0.16. NEEM winter  $\delta^{18}\text{O}$  has no correlation with the Nov-Apr  
275 averaged NAO in 1931-2004. Although the correlation map with SLP shows NAO-like pattern for the 1855-  
276 1930 and the 1855-2004 period, the correlation coefficients with Nov-Apr averaged NAO indices are also rather  
277 weak ( $r=0.217$  for 1855-1930 and  $r=0.191$  for 1855-2004). Furthermore, it should be noted that even if there are  
278 correlations between seasonal NEEM  $\delta^{18}\text{O}$  and AMO and NAO, those circulation patterns can only explain less  
279 than 7% of the variance of NEEM  $\delta^{18}\text{O}$ . We conclude that both patterns exert weak influence on NEEM  $\delta^{18}\text{O}$   
280 even do correlations between seasonal circulation indices and seasonal NEEM  $\delta^{18}\text{O}$ . The weak correlations with  
281 NEEM  $\delta^{18}\text{O}$  are likely due to a larger distance from the Atlantic Ocean and a much lower snow accumulation at  
282 NEEM than other ice cores in central and southern Greenland (Chylek et al., 2012; Steen-Larsen et al., 2011).  
283 The weak correlations can also explain why NEEM annual  $\delta^{18}\text{O}$  is highly correlated with annual Greenland  $\delta^{18}\text{O}$   
284 PC1, but surprisingly weakly correlated with annual and winter NAO (Masson-Delmotte et al., 2015) which  
285 leave a strong footprint in most ice cores in central and southern Greenland (Vinther et al., 2003; Vinther et al.,  
286 2010). The seasonal precipitation bias at NEEM which is dominated by summer precipitation, skews the NEEM  
287 annual average  $\delta^{18}\text{O}$  towards summer. Therefore, the NEEM annual  $\delta^{18}\text{O}$  presents a summer-biased signal which  
288 has strong correlation with Greenland  $\delta^{18}\text{O}$  PC1. Furthermore, irrespective of the weaker winter signal in the  
289 annual  $\delta^{18}\text{O}$ , we also find that the isolated NEEM winter  $\delta^{18}\text{O}$  correlates poorly with winter NAO. This weak  
290 correlation between winter NEEM  $\delta^{18}\text{O}$  and winter NAO is in contrast with the finding of a strong winter NAO  
291 footprint in the winter  $\delta^{18}\text{O}$  records in central/southern Greenland. This is important to know when considering  
292 NEEM  $\delta^{18}\text{O}$  for use in circulation reconstructions using emerging re-analysis techniques (e.g. Hakim et al.,  
293 2016), where a strong seasonality can both be a caveat, but also be exploited for climate reconstructions.

## 294 6.2 Comparison with sea ice concentration

295 In this section, NEEM seasonal  $\delta^{18}\text{O}$  is compared with the SIC record in Baffin Bay for 1901-2004 (Fig.  
296 6). The period is further divided into prior satellite observation period (1901-1978) and satellite observation  
297 period (1979-2004) for comparison. The year 1979 is the onset year of the satellite observations which is  
298 regarded as the more reliable data source. Prior to the satellite period, the data are mainly calculated by the  
299 compilation of historical data (Walsh and Chapman, 2001). SIC data are linearly detrended before correlations  
300 (Fig. 4g). The NEEM winter  $\delta^{18}\text{O}$  correlates significantly with Nov-Apr averaged SIC extent over Baffin Bay in  
301 1979-2004 with correlation coefficients of up to -0.62 (Fig. 6d). The correlation coefficient between NEEM  
302 winter  $\delta^{18}\text{O}$  and averaged SIC over the whole Baffin Bay is -0.53. Prior to the satellite period the correlation  
303 between NEEM winter  $\delta^{18}\text{O}$  and averaged SIC over Baffin Bay is also significant ( $r=-0.27$ ). Summer  $\delta^{18}\text{O}$   
304 correlates well with May-Oct averaged SIC in 1979-2004 with correlation coefficients of up to -0.59 along the  
305 Greenland western coastal area (Fig. 6b). The correlation between NEEM summer  $\delta^{18}\text{O}$  and averaged SIC over





306 Baffin Bay is also significant ( $r=-0.46$ ). However, in contrast to the good correlation in the late 20<sup>th</sup> century,  
307 there are limited significant correlations over the southern part of Baffin Bay for summer in the 1901-1978  
308 period. There is no correlation between NEEM summer  $\delta^{18}\text{O}$  and averaged SIC over Baffin Bay ( $r=-0.04$ ) for  
309 this period. One possible explanation for the weaker correlations both for winter and summer in 1901-1978 may  
310 be due to less reliable historical data sources. Furthermore, the reconstructed summer SIC can be underestimated  
311 sometimes due the lower concentration along the coastlines (Titchner and Rayner, 2014). The correlations with  
312 SIC in 1901-1978 are expected to be re-examined in the future possibly leading to an improved sea ice dataset  
313 (Titchner and Rayner, 2014). But still both winter and summer  $\delta^{18}\text{O}$  are strongly negatively correlated with  
314 Baffin Bay ice extent for 1979-2004 sharing more than 22% variance, which is in agreement with the  
315 relationship between the annual Baffin Bay sea ice anomaly and NEEM annual  $\delta^{18}\text{O}$  data as illustrated in Steen-  
316 Larsen et al. (2011).

317 A possible explanation for the sea ice effect on  $\delta^{18}\text{O}$  is that a reduced sea ice cover may amplify regional  
318 temperature changes and favor enhanced storminess and enhanced precipitation (Noël et al., 2014; Sime et al.,  
319 2013) thus bringing more local moisture. By contrast to the long-distance transport of moisture from the North  
320 Atlantic, the local source leads to less depleted  $\delta^{18}\text{O}$  in the clouds and thereby, increases NEEM  $\delta^{18}\text{O}$ . However,  
321 this mechanism cannot explain the good correlation with winter  $\delta^{18}\text{O}$  as NEEM winter  $\delta^{18}\text{O}$  is poorly correlated  
322 with SAT over the Baffin Bay (Fig. 5b). One hypothesis of this significant winter correlation with SIC may be  
323 attributed to the wind over Baffin Bay. However, we find no correlations between NEEM winter  $\delta^{18}\text{O}$  and Nov-  
324 Apr averaged wind speed/direction at 850mb and 200mb altitude (jet stream) over 1901-1978 and 1979-2004  
325 (not shown), which may exclude this hypothesis. Another possible hypothesis for the winter correlation could be  
326 the climatic connection between sea ice extent and temperatures in clouds affecting the isotopic composition of  
327 the moisture (Steen-Larsen et al., 2011). Future work can focus on investigating the possible driving factors for  
328 this strong winter correlation which is also consistently significant for the early 20<sup>th</sup> century. The strong  
329 correlations with SIC indicate the possible strong influence of sea ice changes on the variability of stable isotope  
330 ratios in northern Greenland. It was found that high  $\delta^{18}\text{O}$  values during the last inter-glacial period (the Eemian  
331 period) could not be achieved in interglacial simulations driven by orbital forcing alone (Sime et al., 2013). Sime  
332 et al. (2013) suggest that sea ice reduction may be the most likely cause of high interglacial  $\delta^{18}\text{O}$  in Greenland  
333 ice cores. This explanation is supported by our study showing that changes in SSTs and sea ice cover are indeed  
334 key to understanding the past changes in Greenland water isotopes.

335

## 336 7 Conclusion

337 The climate signals archived in stable isotopes in ice cores are complex and can be difficult to disentangle  
338 with annual isotope data only, especially for the NEEM ice core with uneven seasonal accumulation. Combining  
339 four NEEM shallow ice cores, we extracted the seasonal  $\delta^{18}\text{O}$  signals at NEEM over the 1855-2004 period,  
340 identifying 30% and 70% of the annual accumulation being representative for winter and summer precipitation,  
341 respectively. The quantifications of the signal to noise ratios indicate that a robust seasonal signal can be  
342 extracted from 4 parallel ice cores at NEEM.



343 NEEM summer  $\delta^{18}\text{O}$  is closely associated with Greenland temperatures. Correlation analysis with 20CR  
344 temperature data indicates strong correlations over the whole of Greenland, the Baffin Bay, and areas as far  
345 south as  $35^\circ$  N. NEEM winter  $\delta^{18}\text{O}$  shows no correlation with Greenland temperatures. The NEEM summer  $\delta^{18}\text{O}$   
346 record, rather than NEEM winter  $\delta^{18}\text{O}$  or NEEM annual average  $\delta^{18}\text{O}$ , has been shown to be the better  
347 temperature proxy in Northwestern Greenland. The NEEM summer  $\delta^{18}\text{O}$  variability is coherent with the  
348 Greenland summer  $\delta^{18}\text{O}$  PC1 (sharing up to 30% variance) while the winter signal is not, which indicate a  
349 seasonal shift in the impact of circulation and large differences in the regional climate signal in Greenland. The  
350 good summer correlations with temperature and Greenland  $\delta^{18}\text{O}$  PC1 agree well with annual correlations which  
351 are however, dominated by the large fraction of summer accumulation. While the strong correlations are not  
352 observed in winter signal. We conclude that the annual  $\delta^{18}\text{O}$  signal is dominated by summer signal at NEEM  
353 where summer precipitation is dominant. At such seasonally precipitation biased sites it is highly desirable to  
354 identify the seasonal  $\delta^{18}\text{O}$  signal even though multiple cores are usually required to minimize the noise.

355 Despite the dominant signals of both NAO and AMO in the southern-central ice core isotope data, we  
356 find that, both these circulation patterns exert only a weak influence on seasonal  $\delta^{18}\text{O}$  variations at NEEM. This  
357 has to be kept in mind when combining NEEM  $\delta^{18}\text{O}$  records with other proxy data in circulation reconstructions.

358 Furthermore, we identify a connection between SIC in Baffin Bay and NEEM summer and winter  $\delta^{18}\text{O}$  in  
359 the satellite SIC data. NEEM winter  $\delta^{18}\text{O}$  shows consistent significant correlations to SIC prior and during the  
360 satellite observation period. This indicates that the NEEM winter  $\delta^{18}\text{O}$  rather than representing temperature itself,  
361 is reflecting sea ice variations and therefore, the distance to the moisture source region. This also opens up for  
362 the possibility of estimating the winter Baffin Bay sea ice extent prior to the onset of satellite observations in  
363 1979 using NEEM winter  $\delta^{18}\text{O}$ .

364



365 **Acknowledge**

366 This work is supported by the scholarship from China Scholarship Council (CSC) under the Grant CSC  
367 No.201606710087. Florian Adolphi was supported by the Swedish Research Council (Grant number VR 4.1-  
368 2016-00218). Raimund Muscheler was also supported by the Swedish Research (Grant Number DNR2013-8421)

369

370 **Reference**

- 371 Barlow, L. K., White, J. W. C., Barry, R. G., Rogers, J. C., and Grootes, P. M.: The North Atlantic Oscillation  
372 signature in deuterium and deuterium excess signals in the Greenland Ice Sheet Project 2 Ice Core, 1840-1970,  
373 *Geophysical Research Letters*, 20, 2901-2904, 10.1029/93gl03305, 1993.
- 374 Cappelen, J.: Greenland-DMI historical climate data collection 1784–2016, Technical Report 17-04, 2017.
- 375 Chylek, P., Folland, C., Frankcombe, L., Dijkstra, H., Lesins, G., and Dubey, M.: Greenland ice core evidence  
376 for spatial and temporal variability of the Atlantic Multidecadal Oscillation, *Geophysical Research Letters*, 39,  
377 n/a-n/a, 10.1029/2012gl051241, 2012.
- 378 Compo, G. P., Whitaker, J. S., Sardeshmukh, P. D., Matsui, N., Allan, R. J., Yin, X., Gleason, B. E., Vose, R. S.,  
379 Rutledge, G., Bessemoulin, P., Brönnimann, S., Brunet, M., Crouthamel, R. I., Grant, A. N., Groisman, P. Y.,  
380 Jones, P. D., Kruk, M. C., Kruger, A. C., Marshall, G. J., Mauerer, M., Mok, H. Y., Nordli, Ø., Ross, T. F., Trigo,  
381 R. M., Wang, X. L., Woodruff, S. D., and Worley, S. J.: The Twentieth Century Reanalysis Project, *Quarterly*  
382 *Journal of the Royal Meteorological Society*, 137, 1-28, 10.1002/qj.776, 2011.
- 383 Ebisuzaki, W.: A Method to Estimate the Statistical Significance of a Correlation When the Data Are Serially  
384 Correlated, *Journal of Climate*, 10, 2147-2153, 10.1175/1520-0442(1997)010<2147:Amets>2.0.Co;2, 1997.
- 385 Gfeller, G., Fischer, H., Bigler, M., Schüpbach, S., Leuenberger, D., and Mini, O.: Representativeness and  
386 seasonality of major ion records derived from NEEM firn cores, *The Cryosphere*, 8, 1855-1870, 10.5194/tc-8-  
387 1855-2014, 2014.
- 388 Hanna, E., Mernild, S. H., Cappelen, J., and Steffen, K.: Recent warming in Greenland in a long-term  
389 instrumental (1881–2012) climatic context: I. Evaluation of surface air temperature records, *Environmental*  
390 *Research Letters*, 7, 045404, 10.1088/1748-9326/7/4/045404, 2012.
- 391 Hirahara, S., Ishii, M., and Fukuda, Y.: Centennial-Scale Sea Surface Temperature Analysis and Its Uncertainty,  
392 *Journal of Climate*, 27, 57-75, 10.1175/jcli-d-12-00837.1, 2014.
- 393 Hurrell, J. W., and Deser, C.: North Atlantic climate variability: The role of the North Atlantic Oscillation,  
394 *Journal of Marine Systems*, 78, 28-41, 10.1016/j.jmarsys.2008.11.026, 2009.
- 395 Johnsen, S. J., Clausen, H. B., Cuffey, K. M., Hoffmann, G., Schwander, J., and Creyts, T.: Diffusion of stable  
396 isotopes in polar firn and ice: the isotope effect in firn diffusion, 2000.
- 397 Küttel, M., Steig, E. J., Ding, Q., Monaghan, A. J., and Battisti, D. S.: Seasonal climate information preserved in  
398 West Antarctic ice core water isotopes: relationships to temperature, large-scale circulation, and sea ice, *Climate*  
399 *Dynamics*, 39, 1841-1857, 10.1007/s00382-012-1460-7, 2012.
- 400 Masson-Delmotte, V., Kageyama, M., Braconnot, P., Charbit, S., Krinner, G., Ritz, C., Guilyardi, E., Jouzel, J.,  
401 Abe-Ouchi, A., Crucifix, M., Gladstone, R. M., Hewitt, C. D., Kitoh, A., LeGrande, A. N., Marti, O., Merkel, U.,  
402 Motoi, T., Ohgaito, R., Otto-Bliesner, B., Peltier, W. R., Ross, I., Valdes, P. J., Vettoretti, G., Weber, S. L.,



- 403 Wolk, F., and Yu, Y.: Past and future polar amplification of climate change: climate model intercomparisons and  
404 ice-core constraints, *Climate Dynamics*, 26, 513-529, 10.1007/s00382-005-0081-9, 2005a.
- 405 Masson-Delmotte, V., Landais, A., Stievenard, M., Cattani, O., Falourd, S., Jouzel, J., Johnsen, S. J., Dahl-  
406 Jensen, D., Sveinbjörnsdóttir, A., White, J. W. C., Popp, T., and Fischer, H.: Holocene climatic changes in  
407 Greenland: Different deuterium excess signals at Greenland Ice Core Project (GRIP) and NorthGRIP, *Journal of*  
408 *Geophysical Research: Atmospheres*, 110, n/a-n/a, 10.1029/2004jd005575, 2005b.
- 409 Masson-Delmotte, V., Steen-Larsen, H. C., Ortega, P., Swingedouw, D., Popp, T., Vinther, B. M., Oerter, H.,  
410 Sveinbjörnsdóttir, A. E., Gudlaugsdóttir, H., Box, J. E., Falourd, S., Fettweis, X., Gallée, H., Garnier, E., Gkinis,  
411 V., Jouzel, J., Landais, A., Minster, B., Paradis, N., Orsi, A., Risi, C., Werner, M., and White, J. W. C.: Recent  
412 changes in north-west Greenland climate documented by NEEM shallow ice core data and simulations, and  
413 implications for past-temperature reconstructions, *The Cryosphere*, 9, 1481-1504, 10.5194/tc-9-1481-2015, 2015.
- 414 Neem community members: Eemian interglacial reconstructed from a Greenland folded ice core, *Nature*, 493,  
415 489-494, 10.1038/nature11789, 2013.
- 416 Noël, B., Fettweis, X., van de Berg, W. J., van den Broeke, M. R., and Erpicum, M.: Sensitivity of Greenland Ice  
417 Sheet surface mass balance to perturbations in sea surface temperature and sea ice cover: a study with the  
418 regional climate model MAR, *The Cryosphere*, 8, 1871-1883, 10.5194/tc-8-1871-2014, 2014.
- 419 Noone, D., and Simmonds, I.: Sea ice control of water isotope transport to Antarctica and implications for ice  
420 core interpretation, *Journal of Geophysical Research: Atmospheres*, 109, n/a-n/a, 10.1029/2003JD004228, 2004.
- 421 Ortega, P., Swingedouw, D., Masson-Delmotte, V., Risi, C., Vinther, B., Yiou, P., Vautard, R., and Yoshimura,  
422 K.: Characterizing atmospheric circulation signals in Greenland ice cores: insights from a weather regime  
423 approach, *Climate Dynamics*, 43, 2585-2605, 10.1007/s00382-014-2074-z, 2014.
- 424 Sime, L. C., Risi, C., Tindall, J. C., Sjolte, J., Wolff, E. W., Masson-Delmotte, V., and Capron, E.: Warm climate  
425 isotopic simulations: what do we learn about interglacial signals in Greenland ice cores?, *Quaternary Science*  
426 *Reviews*, 67, 59-80, 10.1016/j.quascirev.2013.01.009, 2013.
- 427 Steen-Larsen, H. C., Masson-Delmotte, V., Sjolte, J., Johnsen, S. J., Vinther, B. M., Bréon, F. M., Clausen, H. B.,  
428 Dahl-Jensen, D., Falourd, S., Fettweis, X., Gallée, H., Jouzel, J., Kageyama, M., Lerche, H., Minster, B., Picard,  
429 G., Punge, H. J., Risi, C., Salas, D., Schwander, J., Steffen, K., Sveinbjörnsdóttir, A. E., Svensson, A., and White,  
430 J.: Understanding the climatic signal in the water stable isotope records from the NEEM shallow firn/ice cores in  
431 northwest Greenland, *Journal of Geophysical Research*, 116, 10.1029/2010jd014311, 2011.
- 432 Steen-Larsen, H. C., Masson-Delmotte, V., Hirabayashi, M., Winkler, R., Satow, K., Prié, F., Bayou, N., Brun,  
433 E., Cuffey, K. M., Dahl-Jensen, D., Dumont, M., Guillevic, M., Kipfstuhl, S., Landais, A., Popp, T., Risi, C.,  
434 Steffen, K., Stenni, B., and Sveinbjörnsdóttir, A. E.: What controls the isotopic composition of Greenland  
435 surface snow?, *Climate of the Past*, 10, 377-392, 10.5194/cp-10-377-2014, 2014.
- 436 Tang, C. C. L., Ross, C. K., Yao, T., Petrie, B., DeTracey, B. M., and Dunlap, E.: The circulation, water masses  
437 and sea-ice of Baffin Bay, *Progress in Oceanography*, 63, 183-228, 10.1016/j.pocean.2004.09.005, 2004.
- 438 Titchner, H. A., and Rayner, N. A.: The Met Office Hadley Centre sea ice and sea surface temperature data set,  
439 version 2: 1. Sea ice concentrations, *Journal of Geophysical Research: Atmospheres*, 119, 2864-2889,  
440 10.1002/2013jd020316, 2014.
- 441 Trenberth, K. E., and Shea, D. J.: Atlantic hurricanes and natural variability in 2005, *Geophysical Research*  
442 *Letters*, 33, 10.1029/2006gl026894, 2006.



- 443 Vinther, B. M., Johnsen, S. J., Andersen, K. K., Clausen, H. B., and Hansen, A. W.: NAO signal recorded in the  
444 stable isotopes of Greenland ice cores, *Geophysical Research Letters*, 30, 10.1029/2002gl016193, 2003.
- 445 Vinther, B. M., Andersen, K. K., Jones, P. D., Briffa, K. R., and Cappelen, J.: Extending Greenland temperature  
446 records into the late eighteenth century, *Journal of Geophysical Research*, 111, 10.1029/2005jd006810, 2006.
- 447 Vinther, B. M., Jones, P. D., Briffa, K. R., Clausen, H. B., Andersen, K. K., Dahl-Jensen, D., and Johnsen, S. J.:  
448 Climatic signals in multiple highly resolved stable isotope records from Greenland, *Quaternary Science Reviews*,  
449 29, 522-538, 10.1016/j.quascirev.2009.11.002, 2010.
- 450 Walsh, J. E., and Chapman, W. L.: 20th-century sea-ice variations from observational data, *Ann. Glaciol.*, 33,  
451 444-448, 2001.
- 452 Wong, G. J., Osterberg, E. C., Hawley, R. L., Courville, Z. R., Ferris, D. G., and Howley, J. A.: Coast-to-interior  
453 gradient in recent northwest Greenland precipitation trends (1952–2012), *Environmental Research Letters*, 10,  
454 114008, 10.1088/1748-9326/10/11/114008, 2015.

455



**Table 1.** The correlations of seasonal NEM  $\delta^{18}\text{O}$  records with seasonal averaged different atmospheric circulation indices. The bold text is significant at 95 % confidence level, and the text marked with underline is significant at 90% confidence level (T-test).

Time	Correlation			
	NAO		AMO	
	winter	summer	winter	summer
1855-1930	<u>0.217</u>	-0.094	-0.148	<b>0.247</b>
1931-2004	0.059	<b>-0.252</b>	0.148	<b>0.255</b>
1855-2004	<b>0.191</b>	<b>-0.161</b>	-0.053	<b>0.221</b>



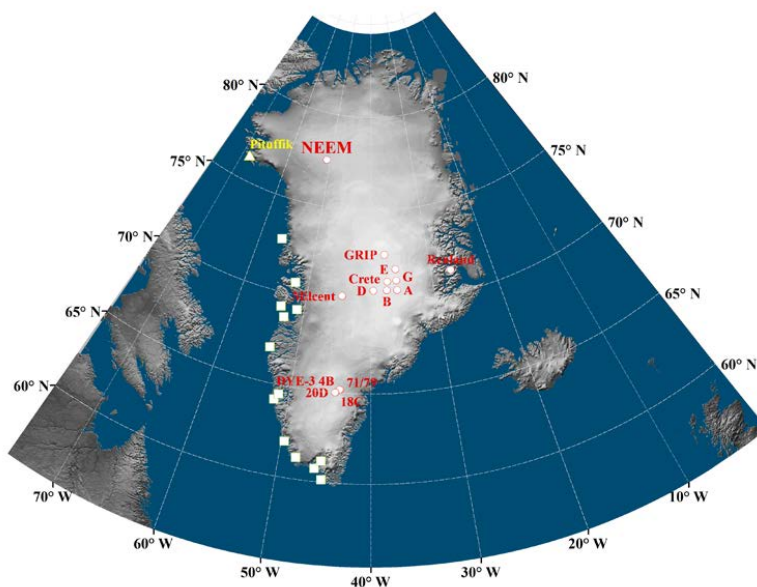
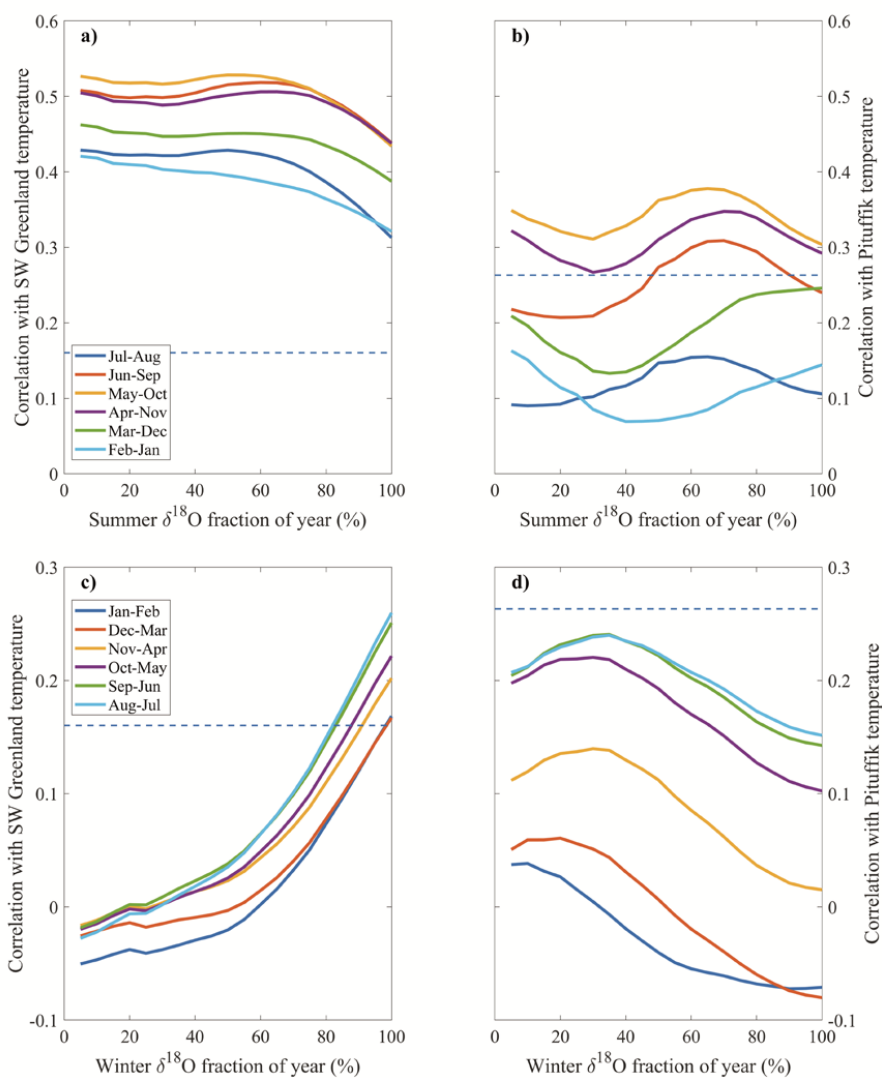
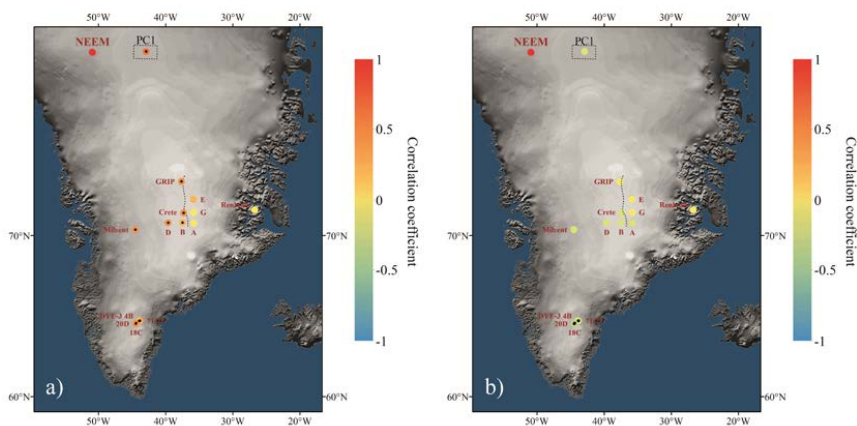


Figure 1. The map of Greenland and ice cores and meteorological stations used for this study. The square indicates the meteorological stations using for SW Greenland temperature series. The Pituffik station is marked as triangle. The ice core sites are shown as circle.



**Figure 2.** Correlation coefficients between stacked data of seasonal  $\delta^{18}\text{O}$  and SW Greenland (a,c) and Pituffik (b,d) measurement temperature records depending on variously defined choices of seasonal  $\delta^{18}\text{O}$  data. The analysis covers 1855-2004 for SW Greenland record and the period 1949-2004 for Pituffik record. The 95% confidence level is marked as dashed line (T-test).



**Figure 3.** Correlation coefficients between NEMM seasonal  $\delta^{18}\text{O}$  and Greenland seasonal  $\delta^{18}\text{O}$  records for the period 1855-1970 (a for summer and b for winter). The PC1 of seasonal central/southern Greenland  $\delta^{18}\text{O}$  records is shown within the black dashed rectangle. The ice divide is marked by dotted black line. The significant correlations at 95% confidence level are filled with black dot (T-test).

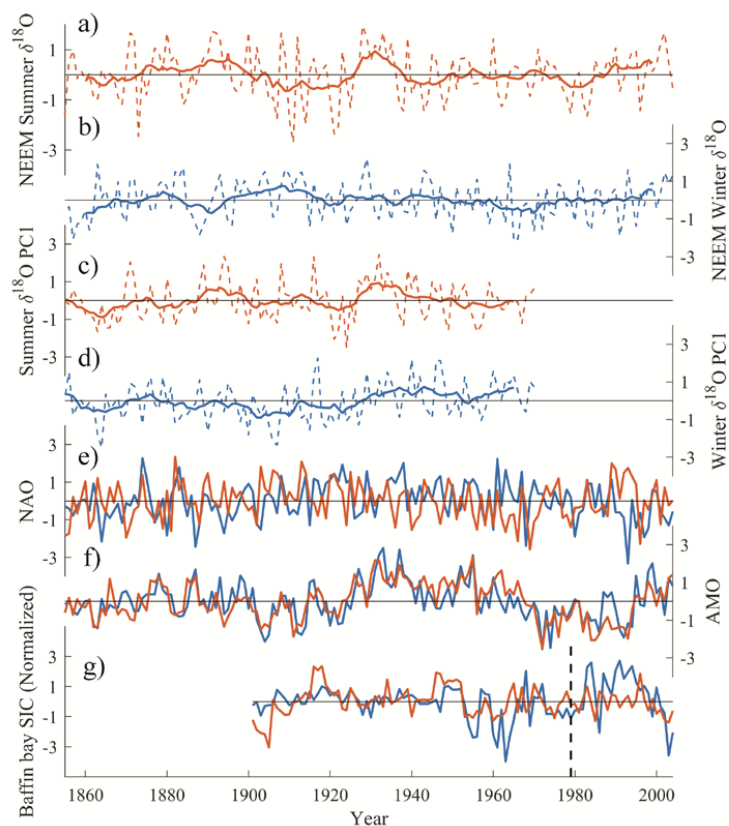


**Figure 4.** a-b) The NEM seasonal  $\delta^{18}\text{O}$  identified in this study. The dashed line and bold line show annual and 11-year averaged data, respectively. c-d) The Greenland seasonal  $\delta^{18}\text{O}$  PC1 extracted from ice cores in Central/Southern Greenland. The dashed line and bold line show annual and 11-year averaged data. e) The NAO indices calculated from 20CR reanalysis data using principal component analysis. f) The AMO indices calculated from 20CR reanalysis data based on the method by Trenberth and Shea (2006). g) The averaged SIC over Baffin Bay extracted from COBESic. The dashed line indicates the start year of satellite observation (1979). All red color lines show summer and blue color lines for winter. All data are normalized and detrended.

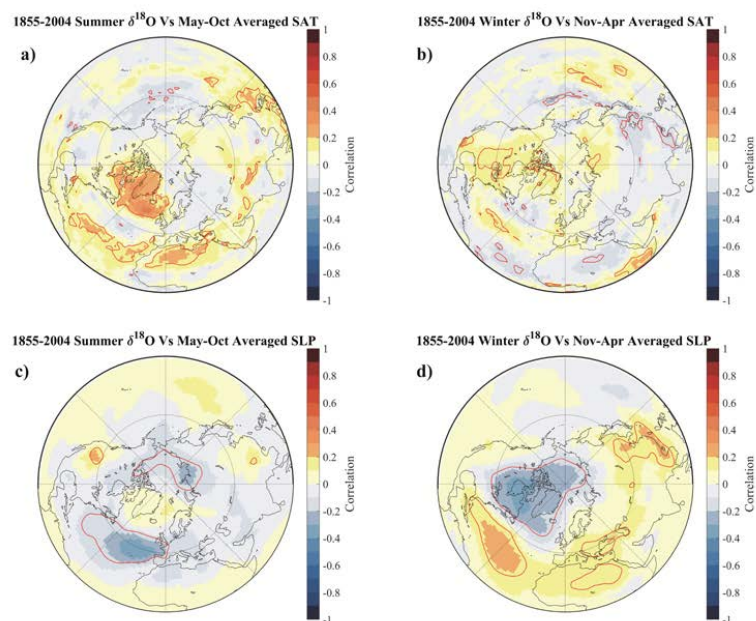


**Figure 5.** The spatial correlation map between NEEM seasonal  $\delta^{18}\text{O}$  and SAT (a,b) and SLP (c,d) from 20CR reanalysis data for the period 1855-2004. The winter data are averaged for Nov-Apr and the summer data are averaged for May-Oct. The red solid lines indicate significant correlation at 95% confidence level (T-test)

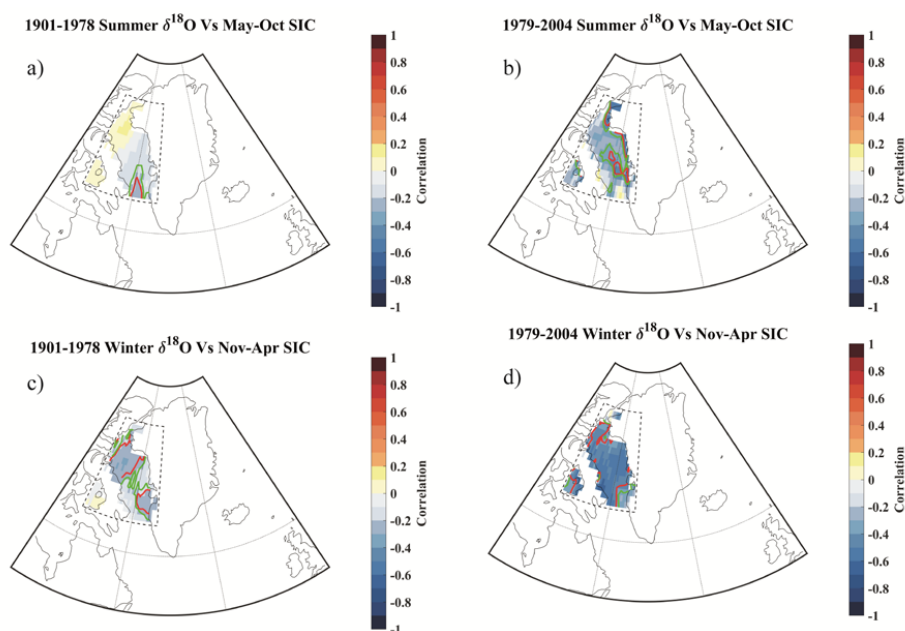


Figure 6. The spatial correlation map between NEEM seasonal  $\delta^{18}\text{O}$  and SIC over Baffin Bay for prior satellite observation period (a,c) and satellite observation period (b,d). The winter data are averaged for Nov-Apr and the summer data are averaged for the May-Oct. The red solid lines indicate significant correlation at 95% confidence level and green solid lines at 90% confidence level (T-test).